applied sciences

MDPI

Article

The Influence of Boiling on the Streamlined Body Drag Force and Falling Velocity

Linas Paukštaitis [1], Sigitas Kilikevičius [2], Ramūnas Česnavičius [3,*], Kristina Liutkauskienė [3] and Tadas Ždankus [4]

[1] Department of Thermal and Nuclear Energy, Kaunas University of Technology, Studentų St. 56, 51424 Kaunas, Lithuania; linas.paukstaitis@ktu.lt
[2] Department of Transport Engineering, Kaunas University of Technology, Studentų St. 56, 51424 Kaunas, Lithuania; sigitas.kilikevicius@ktu.lt
[3] Department of Mechanical Engineering, Kaunas University of Technology, Studentų St. 56, 51424 Kaunas, Lithuania; kristina.liutkauskiene@ktu.lt
[4] Civil Engineering and Architecture Competence Centre, Kaunas University of Technology, Studentų St. 48, 51367 Kaunas, Lithuania; tadas.zdankus@ktu.lt
* Correspondence: ramunas.cesnavicius@ktu.lt

Abstract: This article presents the results of numerical investigation of the influence of the streamlined body temperature on drag force and on the falling velocity in a water channel. The experimental data reflecting the cooling dynamics and body temperature influence on the falling velocity are presented as well. $k-\varepsilon$ turbulence model and homogenous heat transfer model were chosen for the numerical 3D simulation. Drag force changes induced by the alteration of the body temperature were investigated. Velocity of the streamlined body under different temperatures of water was investigated experimentally, and the results were compared to the data obtained during the numerical simulation. The increase of the falling velocity and decrease of drag force were found to have been affected by the increase of the body temperature, which had influence on the change of the water parameters (density, phase, etc.) near the surface of the body. Simulation showed that the drag force and a velocity also depended on the water temperature. The drag force of the streamlined body decreased by 32% in comparison to the cold body for the body temperature equal to 150 °C and water temperature close to the saturation temperature (98 °C). Experimentally, it was determined that the velocity of the streamlined body covered by vapor film depended on the falling time and increased by 10–30%. Velocity difference was very small for the cold and hot bodies at the initial moment of the drop; however, it reached 20% and more after 0.3 s of the falling process.

Keywords: drag force; falling velocity; numerical simulation; cooling process; turbulence model; homogenous heat transfer model

Citation: Paukštaitis, L.; Kilikevičius, S.; Česnavičius, R.; Liutkauskienė, K.; Ždankus, T. The Influence of Boiling on the Streamlined Body Drag Force and Falling Velocity. *Appl. Sci.* **2021**, *11*, 1562. https://doi.org/10.3390/app11041562

Received: 7 January 2021
Accepted: 5 February 2021
Published: 9 February 2021

1. Introduction

Reduction of the body drag, moving in a liquid, is one of the main problems in various areas of the engineering and technology. It was shown that gas introduction between the body and the liquid results in a reduction in the drag force. Cottin-Bizonne et al. [1] demonstrated that the combined effect of wetting properties and surface roughness can be utilized for reduction of the friction drag force. Lauga and Stone [2] studied steady pressure-driven Stokes flow in a circular pipe with the surface containing regions of zero surface shear stress. Steinberger et al. [3] proved that the liquid–gas menisci have a high influence on the solid–fluid interface and can change it from slippery to sticky. Superhydrophobic surfaces for drag reduction were analyzed in papers [4–6]. Thus, to reduce friction drag, the control of menisci is essential. Lee and Kim [7] proposed a method for underwater drag reduction by utilizing a hydrophobic nanostructured surface along by means of self-limiting electrolysis. Another similar method, investigated by Elbing et al. [8] and L'vov

et al. [9], is an injection of the micro bubbles or super cavitation. Decrease of drag force in those cases can be sufficient, slight, negligible, or even negative, depending on the body's size, shape, gas layer morphology, etc. (Vakarelski et al. [10], Linke et al. [11]). Application of the boiling crises (film boiling) may be considered as one of the newest technologies allowing reduction of the body's resistance [10,12–16]. Steam film (layer), generated on a hot body's surface, separates the body from the main volume of the liquid; therefore, a resistance reduces sufficiently and the body's velocity increases.

Vakarelski et al. [10] investigated the velocity of a spherical body falling in electrolyte FC-72 under various body temperatures. The investigation showed that the velocity of the spherical body covered by the steam layer was about 2.5 times higher than the velocity of the cold body. Electrolyte FC-72 has low boiling temperature (60 °C) and very low evaporation heat (88 kJ/kg); therefore, the influence of the film boiling (Leidenfrost effect) on the drag force reduction and increase of the falling velocity was substantial. However, relevant parameters for water are much higher; consequently, the influence of film boiling would be different.

Certain works [12–16] were dedicated to the numerical and experimental investigation of drag force reduction and velocity increase during the falling process of the spherical and cylindrical bodies in water under different body and water temperatures.

Gylys et al. [13] investigated the change of velocity near the cold and hot spherical bodies. The simulation showed that, at the front part of the cold body, the slowdown of water was greater than for the same part of the hot body. The shape of the velocity profile was similar to the shape of a liquid drop on the hydrophilic surface. Drag force was higher than for the hot body, where the shape of the velocity profile was similar to the shape of the liquid drop on the hydrophobic surface (similar to ellipsis). Steam generation on the front part of the hot body determined the liquid flow break-away and, consequently, lower drag force. The shape of the velocity profile at the tail part of the spherical body was also different for the cold and hot bodies. Subject to the viscosity forces, tendency towards compression of the liquid flow at the surface of the cold body, and, therewith, increase of the resistance (drag force) of such body, was observed. In the case of the hot body, the steam isolated the surface from the main flow of the liquid; therefore, the drag force was lower than for the cold body. The highest velocity was registered at the edges of the front part of the cylindrical body, i.e., in the areas where the water flow was pulled away from the body surface. The highest drag force was registered at the front and tail parts of the cylindrical body. Drag force behind trail flow of the body was negative because of the formation of the vortexes in that area. Steam generation at the tail part of the hot cylindrical body caused more intensive abruption of the liquid in that area and, consequently, lower drag force and higher velocity.

Gylys et al. [16] investigated dependence of the falling velocity on the spherical body temperature for the water temperature 14 °C. It was found that the intensive steam generation has a significant influence on the falling velocity. Furthermore, the range of the body surface temperature (300–400 °C) was determined where the falling velocity was the highest. It was found that, for the body surface temperature 150 °C and water temperature close to saturation temperature (98 °C), the drag force decreased for the spherical body by about 25% and for the cylindrical body—by about 9%. Maximum increase of velocity (37–38%) was registered for the sphere with the temperature equal to 650 °C and water temperature close to the saturation temperature (98 °C).

Certain bodies moving in a liquid have a streamlined shape (torpedo, submarine, etc.). Data related to the influence of the streamlined body temperature on its hydrodynamics (drag force, velocity) is absent in literature. Nonetheless, such data could be quite interesting for the scientific and applicable purposes. This article is dedicated to the numerical and experimental investigation of the influence of the streamlined body temperature influence on drag force and on the falling velocity of the body in a water channel.

2. Methodology

A three-dimensional model of the streamlined body was established using SOLIDWORKS program. Dimensions of the streamlined body model were as follows: radius 0.02 m, length 0.12 m (Figure 1a,b).

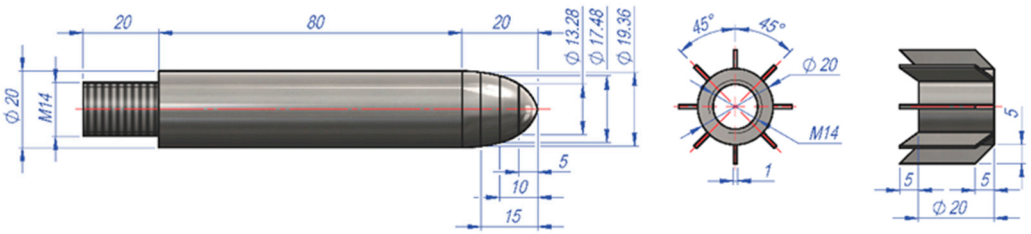

(**a**) (**b**)

Figure 1. Dimensions of the streamlined body: (**a**) body; (**b**) stabilizer.

Simulation was carried out using the CFX module from ANSYS Workbench 15, which applies the Reynolds averaged equations of motion [17]:

$$\frac{\partial \rho}{\partial t} + \frac{\partial}{\partial x_j}(\rho U_j) = 0 \tag{1}$$

$$\frac{\partial \rho U_i}{\partial t} + \frac{\partial}{\partial x_j}(\rho U_i U_j) = -\frac{\partial p}{\partial x_i} + \frac{\partial}{\partial x_j}(\tau_{ij} - \rho\overline{u_i u_j}) + S_M \tag{2}$$

where ρ is the density, U is the vector of velocity, p is the pressure, S_M is the momentum source, τ is the molecular stress tensor, and $\rho\overline{u_i u_j}$ are the Reynolds stresses.

The Reynolds stresses need to be modelled by additional equations of known quantities in order to achieve "closure". The equations used to close the system define the type of turbulence model [17]. The $k-\varepsilon$ turbulence model was used in this study.

The $k-\varepsilon$ turbulence model [17] assumes that the turbulence viscosity is linked to the turbulence kinetic energy and dissipation via the relation:

$$\mu_t = C_\mu \rho \frac{k^2}{\varepsilon} \tag{3}$$

where C_μ is a constant, k is the turbulence kinetic energy, and ε is the turbulence dissipation.

The values of k and ε come directly from the differential transport equations [17] for the turbulence kinetic energy and turbulence dissipation rate:

$$\frac{\partial(\rho k)}{\partial t} + \frac{\partial}{\partial x_j}(\rho U_j k) = \frac{\partial}{\partial x_j}\left[\left(\mu + \frac{\mu_t}{\sigma_k}\right)\frac{\partial k}{\partial x_j}\right] + P_k - \rho\varepsilon + P_{kb} \tag{4}$$

$$\frac{\partial(\rho \varepsilon)}{\partial t} + \frac{\partial}{\partial x_j}(\rho U_j \varepsilon) = \frac{\partial}{\partial x_j}\left[\left(\mu + \frac{\mu_t}{\sigma_\varepsilon}\right)\frac{\partial \varepsilon}{\partial x_j}\right] + \frac{\varepsilon}{k}(C_{\varepsilon 1} P_k - C_{\varepsilon 2}\rho\varepsilon + C_{\varepsilon 1} P_{\varepsilon b}) \tag{5}$$

where μ is the dynamic viscosity, $C_{\varepsilon 1}$, $C_{\varepsilon 2}$, σ_k, and σ_ε are constants. P_{kb} and $P_{\varepsilon b}$ represent the influence of the buoyancy forces, which are described below. P_k is the turbulence production due to viscous forces.

The same modelling approach was adopted in the study as it is presented in [13]. A tetrahedron-type mesh was chosen for application of the finite element method (Figure 2). In order to evaluate the influence of the mesh density on the accuracy of results, a mesh sensitivity analysis was carried out. During the mesh sensitivity analysis, the mesh density was changed from 2 to 10 million elements. The changes in the values of the drag force were insignificant, as the mesh density varied from 6 million to 10 million elements. Near-surface method with inflation layers at the surface of the body (Figure 2) containing

10 million elements was selected for the modeling in order to capture the boundary layer more accurately. The homogenous heat transfer models were chosen for the numerical 3D simulation [13]. The body was placed inside a channel, the outer walls of which were modeled as zero shear walls. Water velocity (v) values from the analyzed range were defined at the channel inlet while the static pressure (p_s) was set to be constant and equal to 0 Pa at the channel outlet. Water temperature was kept close to the boiling temperature; water pressure (p) was equal to 101,325 Pa. The numerical modelling was carried out under the steady state flow regime as this simplification allowed to capture the differences between the velocities of bodies at different temperatures.

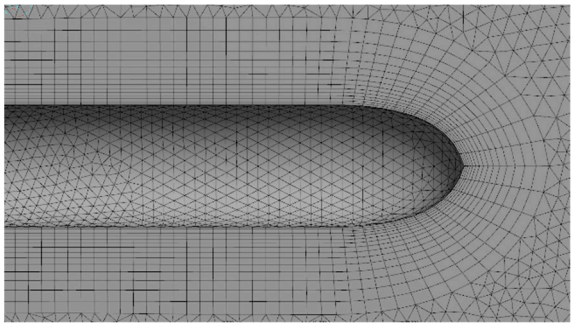

Figure 2. Mesh near the streamline body.

The numerical modeling of the streamlined body was complemented by the results of the experimental investigation. An experimental set-up (Figure 3) was used for that purpose and consisted of a vertical experimental channel, body sample, light source, digital camera, heat source, and computer. The dimensions of the channel were as follows: height 1.55 m; square cross section (0.1 × 0.1) m^2; water level in the channel 1.5 m. The dimensions of the experimental streamlined body sample corresponded to the dimensions used for the numerical investigation (Figure 1a,b). After heating in the electrical furnace (heating device), the body sample was submerged into the channel filled with water from the water-supply system. That particular water was used in order to obtain results applicable to real conditions. The walls of the water channel were made of the transparent material to enable visual observation of the falling process of the body. Body temperature was 98 °C, 150 °C, and 410 °C; water temperature—98 °C. Temperatures of the sample and water were measured by K type thermocouples (measurement range: $-50 \div 750$ °C). One thermocouple (∅0.6 mm) was inserted through the streamlined body and mounted at the distance of 0.5 mm to the opposite surface (front part) of the body and another was installed 50 mm from the center axis of the water tank. Silver paste was used for the sealing and better thermal conductivity k (400 W/(m·K)). Falling velocity of the cold and hot bodies was measured and recorded using Canon EOS 600D camera. The moment of the body's full submerging in the water was taken as a zero time. To reduce the measurement error, all experiments were repeated several times. Deviation of the experimental results varied from 2 to 7%.

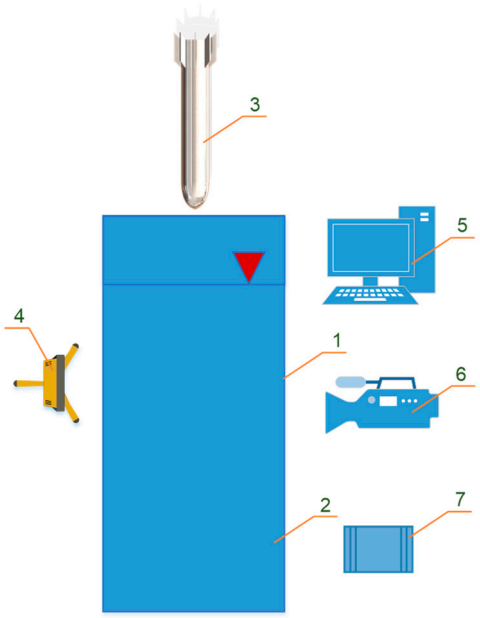

Figure 3. Experimental set-up: 1—channel, 2—water, 3—body, 4—light source, 5—computer, 6—camera, 7—furnace as a heat source for heating up the streamlined body.

3. Results and Discussion

3.1. Results of Simulation

The body at a temperature of 98 °C is relatively referred as the "cold body" while the body at 150 °C is referred as the "hot body". Pressure distribution around the streamlined hot body is shown in Figure 4. The highest pressure was registered at the front part of the body. The closer to the tail, the lower was the pressure, until it was equal to the pressure of a main volume of liquid.

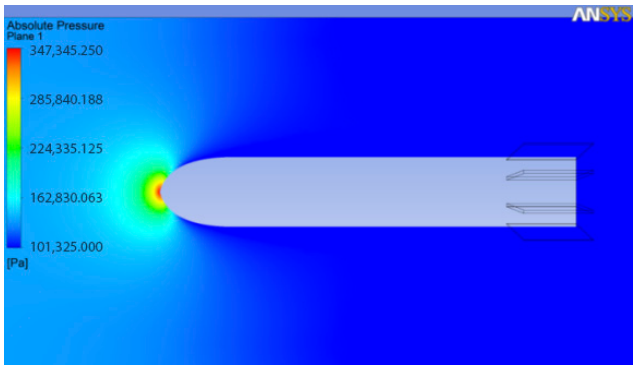

Figure 4. Pressure distribution around the hot streamlined body at 0.5 m/s.

Figure 5 shows the drag force (D) dependence on the body velocity for air and single-phase water flows (right axis refers to water velocity, left axis—air velocity). Air was taken for comparison purposes only. As air velocity was approaching the supersonic velocity, the drag force was growing more intensively due to the air compression near the body surface.

Figure 6 presents the drag coefficient dependence on the body velocity. Numerical modeling was applied for the two cases: body moving in a single-phase liquid (water) and in gas (air).

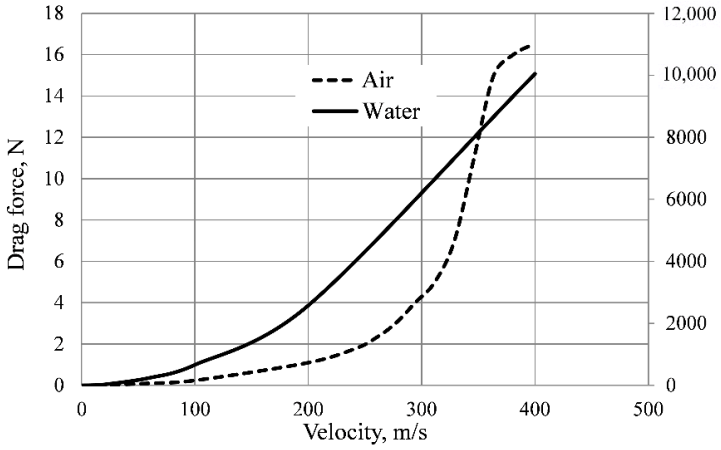

Figure 5. Drag force dependence on the streamlined body velocity.

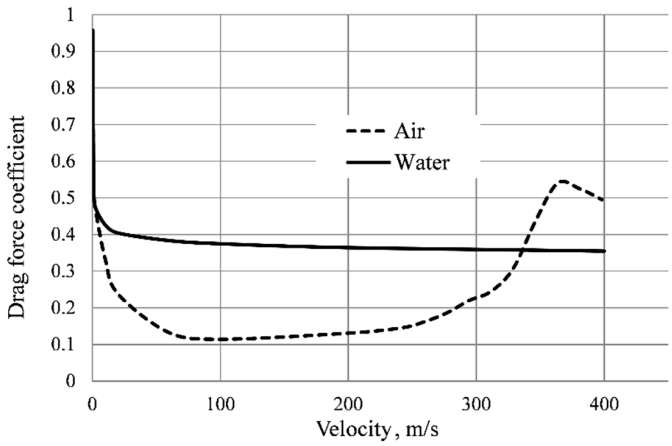

Figure 6. Drag coefficient dependence on the streamlined body velocity.

Figure 7 indicates the distribution of the overflow velocity for the cold (98 °C) and hot (150 °C) bodies. Water flow near the front part and at the tail part of the hot streamlined body was blocked to a lesser extent than in the case of the cold body due to steam formation at the hot body. Consequently, a fluid flow breakaway was observed near the front part and tail of the body. As a result, the drag force was lower for the hot body in comparison to the cold body (Figure 8). Velocity of the liquid phase was the highest at the region where the pressure began to drop (Figure 4).

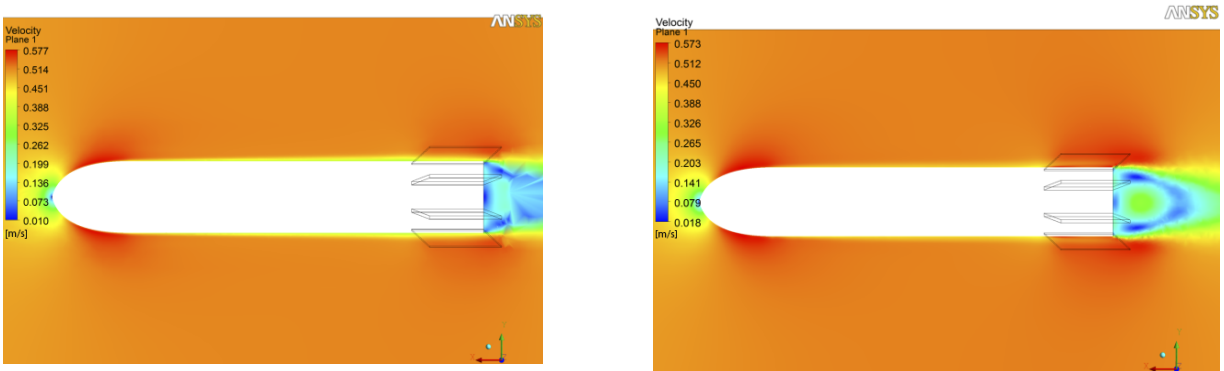

(**a**) (**b**)

Figure 7. Velocity distribution around the cold (**a**) and hot (**b**) streamlined body at 0.5 m/s.

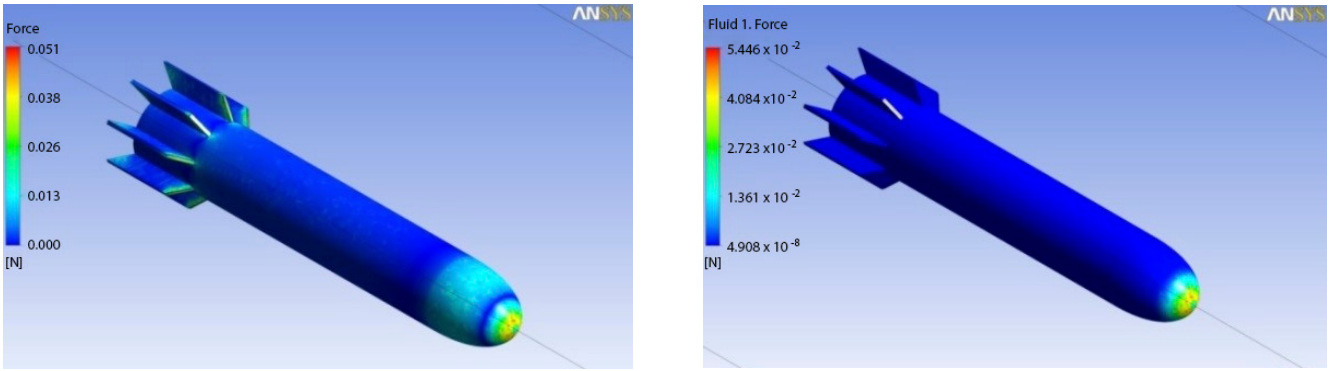

(**a**) (**b**)

Figure 8. Drag force distribution for the cold (**a**) and hot (**b**) streamlined bodies at 0.5 m/s.

Flow of the liquid slowed down more strongly near the front part of the body in the case of the cold body. The shape of the velocity profile was similar to the shape of a liquid drop on a hydrophilic surface. The shape of the velocity profile near the front part of the hot body, different to the spherical and cylindrical bodies, was also similar to the shape of a liquid drop on a hydrophilic surface like in the case of the cold body. However, despite the similarity of the velocity profiles, flow velocity was higher at the surface of the hot body compared to the cold body.

Meanwhile, velocity profile near the tail part of the hot streamlined body was different than in the case of the cold body. The highest velocity was observed near the stabilizer due to presence of the biggest amount of steam at that area. Therefore, the liquid flow was pulled away more intensively at the tail part of the body. In the case of the cold body, the viscosity forces compressed the liquid flow to the whole body and near the tail. All those processes had influence on more intensive stopping of the liquid flow, pressure growth, and drag augmentation of the cold body in comparison to the hot body.

In general, it can be noticed that the streamlined body is particular in that it combines features of motion of the spherical and cylindrical bodies. Steam generation on the front part of the hot body and greater amount of steam near the tail part of the body influenced liquid flow breakaway and, consequently, lower drag force (Figure 8).

Figure 8 shows drag force distribution for the cold and for hot streamlined bodies. It could be noticed that the area of the cold body surface, influenced by the drag force, was larger than that in the case of the hot body. Total value of the drag force was equal to 0.0125 N for the hot body, and 0.0184 N for the cold body. It is clear that steam formation on the surface of the streamlined body resulted in reduction of the drag force like in the case of the spherical or cylindrical bodies [13].

Table 1 presents the modeling results of the streamlined body.

Table 1. Modeling results of the streamlined body.

Body Velocity, m/s	Water Temperature, °C	Body Temperature, °C	Steam Mass Fraction, ω_i	Drag Force D, N	Drag Coefficient C_D
0.5	98	98	0	0.0184	0.417
0.5	98	150	0.004	0.0125	0.283

During the numerical investigation, drag coefficient reduction for the streamlined body was found to be about 32% (from 0.417 for the cold body to 0.283 for the hot body) at body velocity equal to 0.5 m/s.

3.2. Experimental Results

Figures 9–12 show the results of the experimental investigation of the streamlined body cooling process and velocity change.

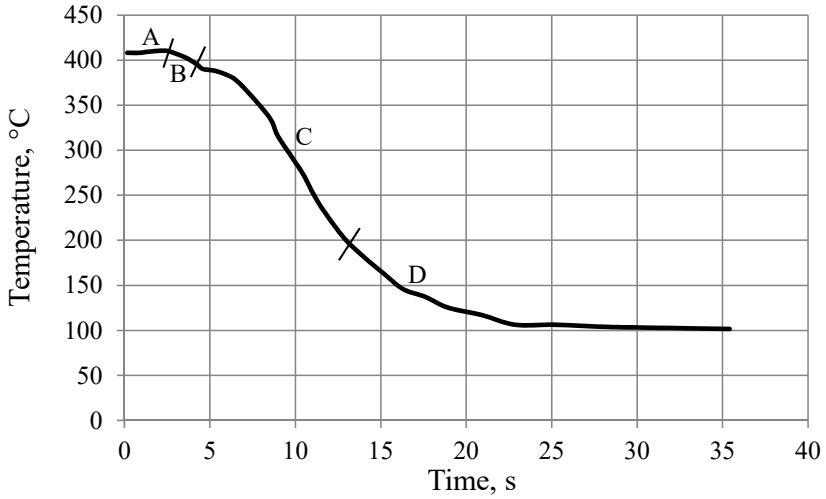

Figure 9. Dynamics of the cooling process of the streamlined body: A—slow cooling in air, B—initial contact with water; C—full immersion in water and film boiling; D—nucleate boiling.

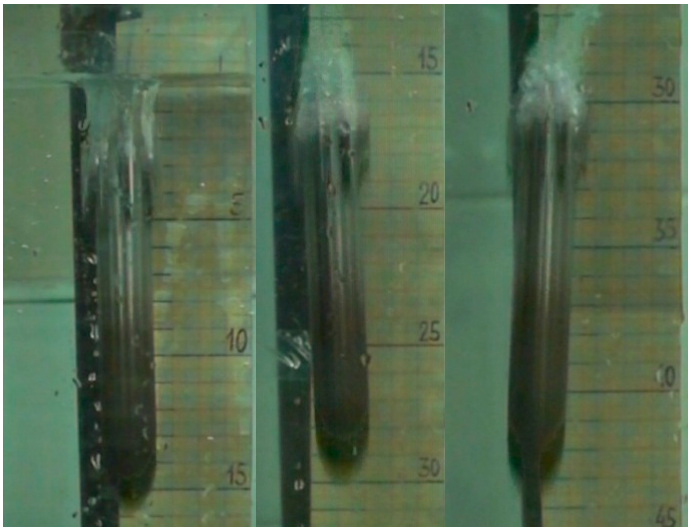

Figure 10. Streamlined hot body positions in different parts of the experimental channel.

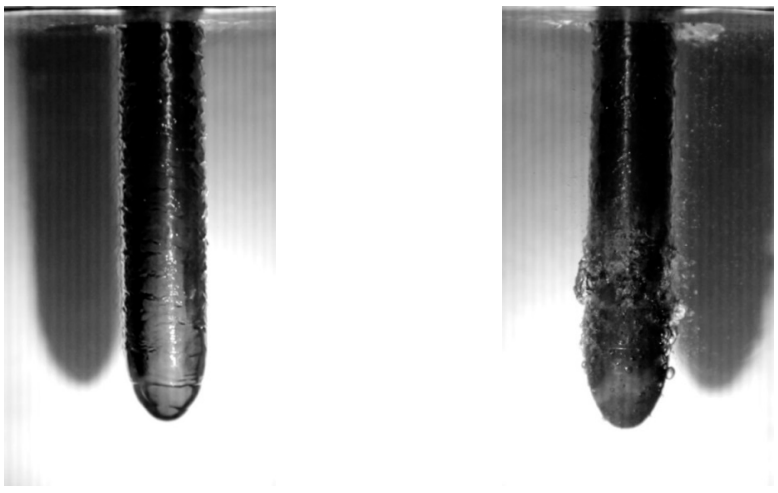

(**a**) (**b**)

Figure 11. Film boiling (**a**) change to nucleate boiling (**b**).

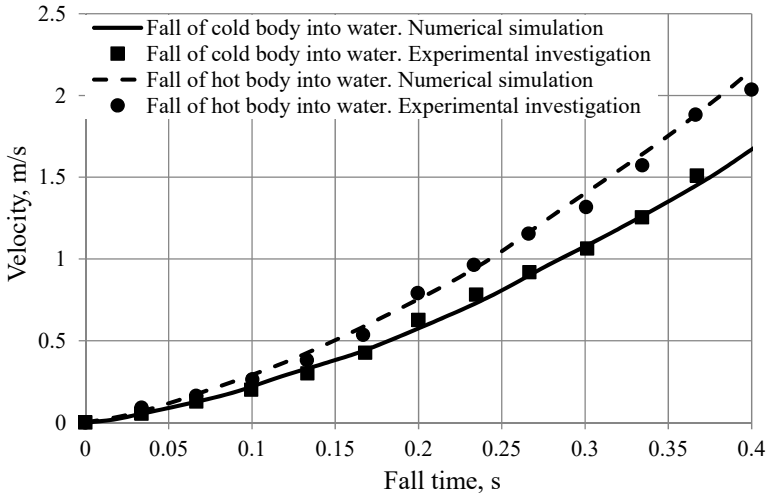

Figure 12. Streamlined body velocity dependence on the falling time.

Figure 9 shows the dynamics of the cooling process of the motionless streamlined body in water, the temperature of which was close to the saturation temperature (98 °C).

Motionless streamlined body was cooled down from 410 °C to 98 °C within 25 s. The investigation showed that the film boiling regime was fully changed by the nucleate boiling regime after 12 s. Meanwhile, for the moving streamlined body, the falling time in water channel was less than 2 s for all the experiments (water column height 1.5 m); therefore, film boiling regime was observed along the entire path of the falling body. Nucleate boiling regime started at the body surface temperature equal to 190 °C.

Figure 10 shows different positions of the hot streamlined body (150 °C) falling in the experimental channel filled with water (98 °C). Intensive steam generation can be noticed at the tail part of the body. Front part of the body was cooled faster due to its permanent contact with the flow of water. Consequently, steam generation occurred here only during the first phase of the contact between the streamlined body and water. The remaining part of the body was in contact with water at a temperature higher than the temperature of main flow due to water heating on the front part of the body. Therefore, steam generation was more intensive and lasted longer at that area.

Figure 11 demonstrates film boiling regime alteration to the nucleate boiling regime. The initial temperature of the streamlined body was 410 °C; water temperature was close to the saturation temperature (98 °C). Film boiling transition to nucleate boiling started at the front part of the body because of the better cooling by the colder water flow contacting the respective part of the body.

Figure 12 demonstrates the streamlined body velocity dependence on the falling time. Due to limitations of the ANSYS CFX program package, the experiments were performed at the body temperature equal to 150 °C and water temperature equal to 98 °C. Such temperatures corresponded to the nucleate boiling regime (Figure 9). Sufficient increase of the body velocity was noticed despite the small amount of vapor generated on the body surface. Solid line and rectangular dots represent the results of the simulation and experimental data correspondingly for the cold body fall in the channel of water (98 °C). Round dots and the dotted line show the experimental data and results of simulation for the hot (150 °C) body falling in water, the temperature of which was 98 °C. Coincidence of the experimental data and the results of simulation were quite good; discrepancy was less than 10%.

It can be noticed that velocity difference was very small for the cold and hot bodies at the initial moment of the fall; however, it reached 20% and more after 0.3 s of the falling process.

4. Conclusions

The article describes the numerical and experimental investigation of the streamlined body temperature influence on the drag force and falling velocity performed.

The investigation showed that the front part of the hot body was cooled faster due to its permanent contact with the flow of water. Steam generation occurred there only during the first phase of the contact between the streamlined body and water.

Film boiling transition to nucleate boiling started from the front part of the body because of better cooling by the colder water flow. The remaining part of the body was in contact with water at a temperature higher than the main flow due to water heating on the front part of the body. Steam generation at the remaining part of the body was more intensive and lasted longer.

Steam generation near the front part and a greater amount of steam near the tail part of the hot body had influence on the liquid flow breakaway and, consequently, on lower drag force in comparison to the cold body. Drag coefficient reduction for the streamlined body was about 32% at the body velocity equal to 0.5 m/s. Velocity of the streamlined body covered by vapor film depended on the falling time and increased by 10–30%. Velocity difference was very small for the cold and hot bodies at the initial moment of the fall; however, it reached 20% and more after 0.3 s of the falling process.

Coincidence of the experimental data and the results of the simulation were quite good; discrepancy was less than 10%.

Author Contributions: Methodology, conceptualization, investigation, funding acquisition: L.P.; methodology, writing—review and editing: S.K.; writing—review and editing, original draft preparation: R.Č., writing—review and editing: K.L.; investigation and methodology: T.Ž. All authors have read and agreed to the published version of the manuscript.

Funding: This research was partially funded by a grant No. 1104 1104MG01 (KETER).

Institutional Review Board Statement: Not applicable.

Informed Consent Statement: Not applicable.

Conflicts of Interest: The authors declare no conflict of interest.

References

1. Cottin-Bizonne, C.; Barrat, J.L.; Bocquet, L.; Charlaix, E. Low-friction flows of liquid at nanopatterned interfaces. *Nat. Mater.* **2003**, *2*, 237–240. [CrossRef] [PubMed]
2. Lauga, E.; Stone, H.A. Effective slip in pressure-driven Stokes flow. *J. Fluid Mech.* **2003**, *489*, 55–77. [CrossRef]
3. Steinberger, A.; Cottin-Bizonne, C.; Kleimann, P.; Charlaix, E. High friction on a bubble mattress. *Nat. Mater.* **2007**, *6*, 665–668. [CrossRef] [PubMed]
4. Borkent, B.M.; Dammer, S.M.; Schönherr, H.; Vancso, G.J.; Lohse, D. Superstability of surface nanobubbles. *Phys. Rev. Lett.* **2007**, *98*, 204502. [CrossRef] [PubMed]
5. McHale, G.; Newton, M.I.; Shirtcliffe, N.J. Immersed superhydrophobic surfaces: Gas exchange, slip and drag reduction properties. *Soft Matter* **2010**, *6*, 714–719. [CrossRef]
6. Rothstein, J.P. Slip on superhydrophobic surfaces. *Annu. Rev. Fluid Mech.* **2010**, *42*, 89–109. [CrossRef]
7. Lee, C.; Kim, C.J. Underwater restoration and retention of gases on superhydrophobic surfaces for drag reduction. *Phys. Rev. Lett.* **2011**, 106014502. [CrossRef] [PubMed]
8. Elbing, B.R.; Winkel, E.S.; Lay, K.A.; Ceccio, S.L.; Dowling, D.R.; Perlin, M. Bubble-induced skin-friction drag reduction and the abrupt transition to air-layer drag reduction. *J. Fluid Mech.* **2008**, *612*, 201. [CrossRef]
9. L'vov, V.S.; Pomyalov, A.; Procaccia, I.; Tiberkevich, V. Drag reduction by microbubbles in turbulent flows: The limit of minute bubbles. *Phys. Rev. Lett.* **2005**, *94*, 174502. [CrossRef] [PubMed]
10. Vakarelski, I.U.; Marston, J.O.; Chan, D.Y.; Thoroddsen, S.T. Drag reduction by Leidenfrost vapor layers. *Phys. Rev. Lett.* **2011**, *106*, 214501. [CrossRef] [PubMed]
11. Linke, H.; Alemán, B.J.; Melling, L.D.; Taormina, M.J.; Francis, M.J.; Dow-Hygelund, C.C.; Narayanan, V.; Taylor, R.P.; Stout, A. Self-propelled Leidenfrost droplets. *Phys. Rev. Lett.* **2006**, *96*, 154502. [CrossRef] [PubMed]
12. Gylys, J.; Skvorčinskienė, R.; Paukštaitis, L. Peculiarities of the Leidenfrost effect application for drag force reduction. *Mechanics* **2014**, *20*, 266–273. [CrossRef]
13. Gylys, J.; Paukštaitis, L.; Skvorčinskienė, R. Numerical investigation of the drag force reduction induced by the two-phase flow generating on the solid body surface. *Int. J. Heat Mass Transf.* **2012**, *55*, 7645–7650. [CrossRef]

14. Vakarelski, I.U.; Patankar, N.A.; Marston, J.O.; Chan, D.Y.; Thoroddsen, S.T. Stabilization of Leidenfrost vapour layer by textured superhydrophobic surfaces. *Nature* **2012**, *489*, 274–277. [CrossRef] [PubMed]
15. Vakarelski, I.U.; Chan, D.Y.; Thoroddsen, S.T. Leidenfrost vapour layer moderation of the drag crisis and trajectories of superhydrophobic and hydrophilic spheres falling in water. *Soft Matter* **2014**, *10*, 5662–5668. [CrossRef] [PubMed]
16. Gylys, J.; Skvorcinskiene, R.; Paukstaitis, L.; Gylys, M.; Adomavicius, A. Water temperature influence on the spherical body's falling velocity. *Int. J. Heat Mass Transf.* **2015**, *89*, 913–919. [CrossRef]
17. Ansys, C.F. *Release 11.0: ANSYS CFX-Solver Theory Guide*; ANSYS Inc.: Canonsburg, PA, USA, 2010.